The Peripheral Neuropathy-Linked *Trembler* and *Trembler-J* Mutant Forms of Peripheral Myelin Protein 22 Are Folding-Destabilized[†]

Jeffrey K. Myers,[‡] Charles K. Mobley,[§] and Charles R. Sanders*

Department of Biochemistry and Center for Structural Biology, Vanderbilt University Medical Center, Nashville, Tennessee 37232-8725

Received June 19, 2008; Revised Manuscript Received August 18, 2008

ABSTRACT: Dominant mutations in the tetraspan membrane protein peripheral myelin protein 22 (PMP22) are known to result in peripheral neuropathies such as Charcot-Marie-Tooth type 1A (CMT1A) disease via mechanisms that appear to be closely linked to misfolding of PMP22 in the membrane of the endoplasmic reticulum (ER). To characterize the molecular defects in PMP22, we examined the structure and stability of two human disease mutant forms of PMP22 that are also the basis for mouse models of peripheral neuropathies: G150D (*Trembler* phenotype) and L16P (*Trembler-J* phenotype). Circular dichroism and NMR spectroscopic studies indicated that, when folded, the three-dimensional structures of these disease-linked mutants are similar to that of the folded wild-type protein. However, the folded forms of the mutants were observed to be destabilized relative to the wild-type protein, with the L16P mutant being particularly unstable. The rate of refolding from an unfolded state was observed to be very slow for the wild-type protein, and no refolding was observed for either mutant. These results lead to the hypothesis that ER quality control recognizes the G150D and L16P mutant forms of PMP22 as defective through mechanisms closely related to their conformational instability and/or slow folding. It was also seen that wild-type PMP22 binds Zn(II) and Cu(II) with micromolar affinity, a property that may be important to the stability and function of this protein. Zn(II) was able to rescue the stability defect of the Tr mutant.

Peripheral myelin protein 22 (PMP22)[1] is a 160-residue integral membrane protein with four putative transmembrane spans. PMP22 is a major protein of the peripheral nervous system myelin (*1, 2*), where it is known to play important roles in regulating Schwann cell proliferation and in myelin formation and maintenance (*3, 4*). A high-resolution structure is yet to be determined for PMP22, although some of its general structural and topological features have been established (*5, 6*). PMP22 represents the PMP22/EMP/MP20/Claudin superfamily [pfam00822 in NCIB (*7*)], which share both sequence homology and their predicted tetraspan topology. PMP22 and some of these other proteins are found at specialized membrane junctions found in myelin and in epithelia (*8*−*11*).

PMP22 is highly expressed in Schwann cells and represents 2−5% of the total protein content of the myelin membrane. Changes in gene dosage or dominant missense mutations in the gene encoding PMP22 result in several inherited peripheral neuropathies (*12*), including hereditary neuropathy with liability to pressure palsies (HNPP), Dejerine-Sottas syndrome (DSS), and Charcot-Marie-Tooth type 1A (CMT1A) disease, the latter being the most common inherited disorder of the peripheral nervous system. For those phenotypes that are caused by missense mutation-encoded changes in PMP22's amino acid sequence, disease is believed to be caused by misassembly of the protein, resulting both in loss of PMP22's normal functions and in toxic "gain of function" that is associated with the accumulation of misassembled protein in the cytosol (*13*−*15*) and, possibly, also in the endoplasmic reticulum (cf., ref *16*).

Two of the several dozen known disease-linked mutant forms of human PMP22, G150D and L16P, have also been discovered as naturally occurring mutations that result in mouse models of peripheral neuropathies, the *Trembler* (Tr, G150D) and *Trembler-J* (TrJ, L16P) phenotypes (*13*). Heterozygous (WT/mutant) mice with these mutations exhibit severely defective myelin and PNS dysfunction very similar to what is observed in humans born with the same mutations

[†] This study was supported by grants from the Muscular Dystrophy Association (MDA3702 to J.K.M. and a pilot grant to C.R.S.) and by the National Institutes of Health (R21 N5048573 and R01 GM47485 to C.R.S.).

* To whom correspondence should be addressed. E-mail: chuck.sanders@vanderbilt.edu. Phone: (615) 936-3756. Fax: (615) 936-2211.

[‡] Current address: Department of Chemistry, Davidson College, Box 7120, Davidson, NC 28035-7120.

[§] Current address: Complex Carbohydrates Research Center, The University of Georgia, Athens, GA 30602-4712.

[1] Abbreviations: CMT1A, Charcot-Marie-Tooth type 1A; CD, circular dichroism; DPC, dodecylphosphocholine; DSS, Dejerine-Sottas syndrome; ER, endoplasmic reticulum; ERAD, ER-associated protein translocation/degradation pathway; HNPP, hereditary neuropathy with liability to pressure palsies; IMAC, immobilized metal ion affinity chromatography; LS, laurylsarcosine; MAG, myelin-associated glycoprotein; MBP, myelin basic protein; MPZ, myelin protein zero; NMR, nuclear magnetic resonance; PMP22, peripheral myelin protein 22; PNS, peripheral nervous system; SDS, sodium dodecyl sulfate; TDPC, tetradecylphosphocholine; TM, transmembrane; Tr, mutation in PMP22 (G150D) linked to human CMT1A and responsible for the *Trembler* mouse phenotype; TrJ, mutation in PMP22 (L16P) linked to human DSS and responsible for the *Trembler-J* mouse phenotype; WT, wild type.

10.1021/bi801157p CCC: $40.75
Published on Web 09/17/2008

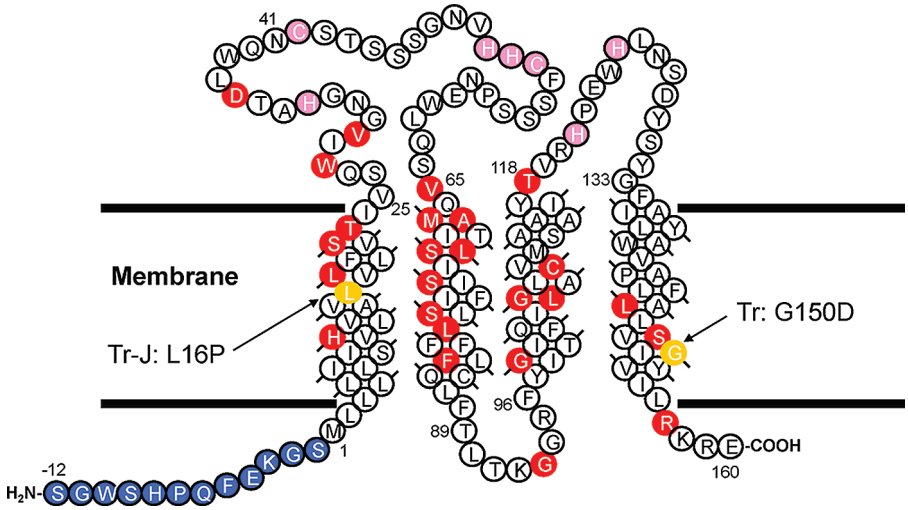

FIGURE 1: Amino acid sequence of human PMP22. Sites of disease-linked point mutations are colored red, residues added to the N-terminus as part of a purification tag blue, and the locations of possible metal ion-coordinating side chains in the extracellular loops pink. The locations of the two disease-linked mutations studied in this work are colored gold.

(severe CMT1A and DSS for the Tr and TrJ mutations, respectively) (*17, 18*). Both of these mutants are recognized as being folding-defective by the quality control system of the endoplasmic reticulum and are targeted for translocation to the cytosol for intended degradation via the ubiquitination/proteasomal pathway, with the autophagy/lysosomal degradation pathway serving as a backup (*13, 14, 17, 19*−*27*). However, it is believed that under disease conditions the loss of function that accompanies the misassembly of these proteins is complicated by toxic accumulation of the misfolded protein in the ER and/or in the cytosol. It is most likely this latter phenomenon and also the ability of these mutants to trigger misfolding of PMP22 encoded by the wild-type allele (via mutant/WT dimerization) that underlies the gain of function component of neuropathy caused by these mutations (*15, 19, 26, 28*).

While previous studies of the mistrafficking of WT and mutant forms of PMP22 represent a body of work that is clear and elegant, little is known about the nature of the defect in newly translated/ER-translocated PMP22 that is recognized and deemed by ER quality control as aberrant. In this paper, we probe this issue by comparing the structure, folding, and stability of wild-type PMP22 to the G150D (Tr) and L16P (TrJ) mutant forms of the protein. Defects in the basic physical properties of these mutants are documented that may well resemble the defects that are recognized by ER quality control.

A second focus of this paper is characterization of PMP22's affinity for divalent metal ions. Previous studies have suggested that PMP22 has an affinity for divalent metal ions such as Cu(II) and Ni(II). PMP22 can be purified from native membranes using Cu(II)-based metal ion affinity chromatography (*29, 30*) and, in our hands, also binds avidly to Ni(II)-chelate resin at pH >6 (unpublished observations). Although Zn(II) and other metal ions have been studied in the central nervous system (*31, 32*), less is known about their role in the peripheral nervous system. Zn(II) has profound effects on the gross structure of myelin, and zinc deficiency in rats is found to cause symptoms very similar to peripheral neuropathy (*33, 34*). Several other proteins of the myelin sheath have been found to be Zn(II) binding proteins (*35*−*37*). We have therefore tested whether PMP22 specifically binds divalent metal cations.

MATERIALS AND METHODS

Protein Expression and Purification. Detailed protocols for the overexpression and purification of PMP22 are given elsewhere (*6*). Briefly, PMP22 was produced as a fusion protein with the first 76 residues of λ repressor, with an intervening polyhistidine tag followed by a TEV protease site and a STREP tag used as a spacer between the beginning of PMP22 and the protease site. Expression was performed in *Escherichia coli* under the control of an IPTG-inducible promoter in minimal medium at 20 °C. The fusion protein was extracted from the membrane with the detergent Empigen (Sigma) and isolated by Ni(II) ion affinity chromatography. While bound to the Ni(II) column, Empigen was replaced by the detergent dodecylphosphocholine (DPC, Anatrace). Cleavage of the fusion protein in DPC micelles was performed with TEV protease, and the mixture was purified by ion exchange chromatography using a Mono S cation exchange column, during which DPC was often replaced by another detergent, tetradecylphosphocholine (TDPC, Anatrace). PMP22 was stored at 5−10 mg/mL at 4 °C, with 10 mM DTT being added to prevent oxidation of the cysteines leading to a disulfide-bonded dimer.

Buffers used in the non-NMR studies of this work were 25 mM sodium acetate at pH 5.5 and 25 mM HEPES at pH 7.5, with 150 mM NaCl present in each. All samples contained micelles of DPC (0.2−0.5%) or TDPC (0.2%). Before divalent metal ion binding experiments, the protein was treated with 1 mM EDTA, followed by removal of the EDTA and DTT by desalting using BioGel P4 resin (Bio-Rad). Samples were used immediately to avoid oxidation of the cysteines.

Fluorescence and Binding Experiments. Fluorescence experiments were performed on a Jobin Yvonne SPEX Fluoromax-3 instrument with a water bath temperature controller and magnetic stirrer at 20 °C. Emission spectra were acquired with excitation at 280 nm and a slit width of 2 nm. Buffer blanks were subtracted from each spectrum.

Divalent cation titrations were performed by serial addition to the stirred solution, with equilibration for 5 min and data collection for 1 min at 340 nm for each point. The average signal was then corrected for the effect of dilution. The following equation was fit to the titration data to extract the binding constant:

$$F = F_a + (F_b - F_a)[[L]/([L] + K_d)] \quad (1)$$

where F stands for the observed fluorescence signal, F_a is the unliganded signal, F_b is the saturated signal, [L] is the free ligand concentration, and K_d is the dissociation constant. A single-binding site model did not give adequate fits for binding of Zn at pH 7 and the binding of Cu; in these cases, the following model was used that assumes either sequential binding to two independent sites or random binding to two sites that have very different affinities.

$$F = (F_a + F_b K_{a1}[L] + K_{a1}K_{a2}[L]^2 F_c)/ (1 + K_{a1}[L] + K_{a1}K_{a2}[L]^2) \quad (2)$$

where K_{a1} and K_{a2} are the association constants, F_a is the fluorescence of the unliganded protein, F_b is the fluorescence of the singly bound protein, and F_c is the fluorescence of the doubly bound protein. Equations 1 and 2 were found to adequately fit all of the titration data collected.

Circular Dichroism. Circular dichroism (CD) experiments were performed on a Jasco J-810 instrument with a Peltier temperature controller and a magnetic stirrer. Samples were placed in either 1 or 0.1 cm path length quartz cuvettes (Hellma). Spectra were acquired at 20 °C with a 1.5 nm bandwidth, averaging for 4 s at each wavelength. Three spectra were averaged together to give the final trace, and blank spectra were subtracted. Protein concentrations were 10 μM in a 0.1 cm cell for far-UV CD or 26 μM in a 1 cm cell for near-UV CD. Thermal denaturation curves were obtained at a CD scan rate of 1 °C/min. Unfolding titrations with the denaturing detergents SDS and laurylsarcosine (LS) were performed by serial addition of each detergent into DPC micellar solutions of PMP22 at 37 °C, with equilibration for 10 min before the collection of near-UV CD data. Ten minutes was observed to be sufficient for the CD intensity at 299 nm to reach a constant value.[2] Data were corrected for the increase in sample volume caused by the additions. A two-state model was fit to the unfolding data to give the curves shown in the figures (*38*).

CD was also used to monitor the unfolding−refolding kinetics of PMP22. The protein in DPC micelles was unfolded by adding LS and then refolded by adding excess DPC. Data were corrected for the increase in sample volume caused by the additions. A single-exponential kinetic model was fit to the refolding data.

[2] The signal during the titrations appears to equilibrate faster than it should judging from the folding kinetics in Figure 3C. However, at least four rate constants (two folding, one unfolding, and one irreversible unfolding) will contribute to the equilibration time, and they will all depend on LS concentration. Thus, it is impossible to judge how long the equilibration should take on the basis of the refolding kinetics presented in Figure 3. PMP22 (un)folding is not a simple two-state process, despite the fact that the titrations appear sigmoidal. Further experimentation is necessary to dissect the contributions of the various rate constants to the kinetics and to determine their dependence on LS.

NMR Experiments. All NMR experiments were carried out using a Bruker Avance 800 MHz spectrometer equipped with a 5 mm CPTCI-Z cryoprobe at a sample temperature of 45 °C. NMR data were collected using the Weigelt version of the $^1H-^{15}N$ TROSY pulse sequence (*39*). PMP22 for NMR samples was ^{15}N-labeled and purified into pH 5.0 TDPC micelles as described previously (*6*). The final concentration of the G150D mutant PMP22 NMR sample was 0.9 mM. The concentration of the L16P mutant PMP22 sample was 1.0 mM. TROSY spectra were acquired for both of these samples in 3 mm diameter NMR tubes (Wilmad), which required the use of adapters (Norrell) to fit into the 5 mm spinner.

RESULTS

Human PMP22 was overexpressed in *E. coli* followed by purification of the protein, a process that includes steps in which the protein is unfolded by harsh detergents followed by refolding in DPC or TDPC micelles, conditions under which the protein has been shown to be a stably folded and largely α-helical homodimer (*6*).

Binding of Zn(II) and Other Divalent Cations to PMP22. We investigated whether PMP22 can bind Zn(II) or other common divalent cations. Fluorescence spectra utilizing intrinsic tryptophan and tyrosine fluorescence are shown in Figure 2. In the presence of 1 mM Zn(II), the fluorescence emission intensity increases by ~20%, and the wavelength of maximal emission decreases slightly. In the presence of 1 mM Cu(II), the intensity dramatically decreases and the wavelength of maximal emission increases slightly. No significant change in the fluorescence spectrum is observed in the presence of Ca(II) or Mg(II) (Figure 2A). Either these metals do not have any significant affinity for PMP22, or (less likely) their binding does not induce any changes in the fluorescence emission spectrum.

In panels B and C of Figure 2, binding isotherms are shown for direct titration of PMP22 with divalent metal cations, as followed by fluorescence. At pH 5.5, Zn(II) binding fits well to a model with a single binding site, with a modest K_d of 1.4 mM. The titrations with Zn(II) near neutral pH or Cu(II) at pH 5.5 exhibit higher affinity. However, neither isotherm is well fit by a simple one-site binding model; a model with two binding sites is necessary to account for the data. The stronger of the two binding constants is 20 μM for Zn(II) and 37 μM for Cu(II), with the second ion binding with millimolar avidity in both cases. The pronounced pH dependence of Zn(II) binding from pH 5.5 to 7.5 is consistent with histidine and/or cysteine side chains being involved as coordinating ligands. The observed micromolar dissociation constant of PMP22 for Zn(II) at neutral pH is close to the Zn(II) binding constants found for certain other myelin proteins (*35*−*37*).

We probed possible conformational changes resulting from Zn(II) binding using circular dichroism (CD). PMP22 is clearly a mostly helical protein as judged from the far-UV CD spectrum shown in Figure 3A (see also ref *6*). The near-UV CD spectrum indicates a well-ordered tertiary structure (Figure 3B). CD data also show that binding of Zn(II) has structural consequences. While scans taken in the presence of Zn(II) exhibit only very small changes in the far-UV spectrum, there is a significant change in the near-UV CD

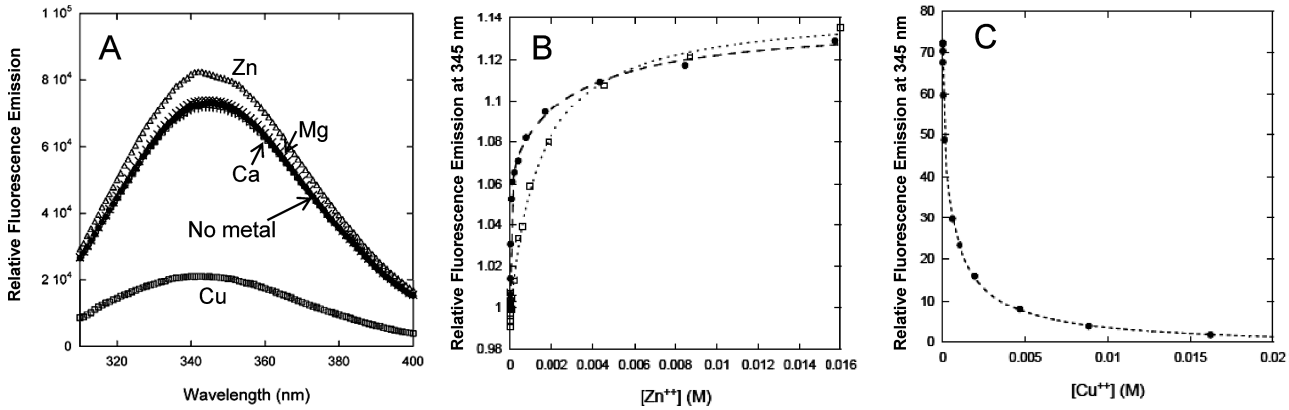

FIGURE 2: PMP22 binds Cu(II) and Zn(II) at 20 °C. (A) Fluorescence emission spectra of PMP22 in DPC micelles in the presence of various metal ions. The protein and metal ion concentrations were 1 μM and 1 mM, respectively. The buffer consisted of 25 mM acetate (pH 5.5), 150 mM NaCl, and 0.5% DPC. (B) Titration with zinc acetate at pH 5.5 (□) and in HEPES buffer at pH 7.5 (●). Single- and double-binding site models were fit to the data to determine dissociation constants (see Materials and Methods). Fitted K_d values for Zn(II) binding were 1.4 mM at pH 5.5 and 20 μM and 3 mM at pH 7.5. (C) Titration with copper sulfate at pH 5.5. Fitted K_d values were 37 μM and 1.1 mM.

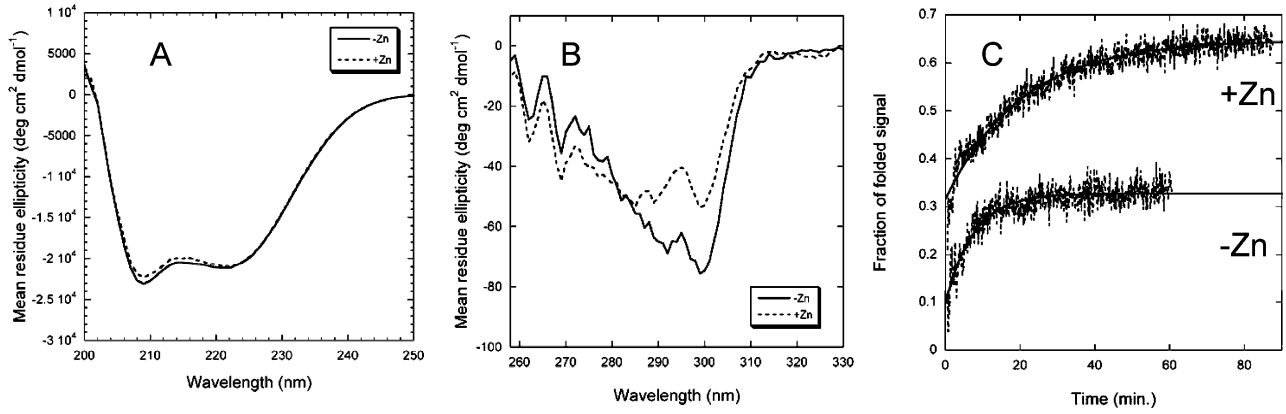

FIGURE 3: Effect of Zn(II) on the structure and folding of wild-type PMP22 as probed by circular dichroism. The buffer included 25 mM acetate (pH 5.5), 150 mM NaCl, and 0.5% DPC, while the Zn(II) concentration was 10 mM in each experiment denoted with dotted lines. (A) Far-UV CD at 25 °C, where the protein concentration in DPC micelles was 10 μM in a 0.1 cm path length cuvette. (B) Near-UV CD at 25 °C, where the protein concentration in DPC micelles was 26 μM in a 1 cm path length cuvette. (C) Kinetics of refolding of PMP22 at 37 °C from a DPC/LS detergent mixture in the absence (black) and presence (gray) of 10 mM Zn(II). Tertiary structure formation was monitored by CD at 299 nm. Black lines are for single-exponential fits of the data.

spectrum. We interpret this data as indicating that there is little change in the helical secondary structure in response to coordination of Zn(II) to PMP22, but that there is some change in the tertiary packing involving one or more aromatic residues. The changes in the near-UV CD spectra are most pronounced in the 290−300 nm range where PMP22's tryptophan side chains are expected to predominate. This indicates that Zn(II) most likely induces a rearrangement in the extracellular loops where four of five of PMP22's tryptophan residues reside, and where multiple His/Cys are located that are likely to dominate Zn(II) binding.

Assessment of the Stability of Wild-Type PMP22. The folding and stability of PMP22 were investigated by unfolding experiments in which harsh detergents were employed as denaturing agents in place of traditional chemical denaturants such as urea or guanidine hydrochloride for use with membrane proteins (*40, 41*).[3] This general approach has been extensively used to probe membrane protein conformational stability (*42*−*46*). The resulting denaturation curves are typically sigmoidal. The well-known two-stage model sets a basic framework for understanding helical membrane protein folding (*47*), but reality is more complex.

It was observed that the tertiary structure of PMP22 in DPC micelles can be unfolded by addition of sodium dodecyl sulfate (SDS) or laurylsarcosine (LS). Time-resolved kinetic unfolding and folding experiments were performed by forward and reverse titrations of folded PMP22 with SDS or LS. At 20 °C unfolding by the addition of SDS to a high mole percentage in the micelles occurs over a time scale of tens of minutes, with an unfolding curve that is best fit by a double exponential (not shown). This suggests that an unfolding intermediate is involved. Attempts to then refold PMP22 (monitored by the return of the original CD signal) by addition of excess mild detergent (DPC) were not successful at 20 °C or at other temperatures. Unfolding using LS at 20 °C proceeds in a manner similar to that of the SDS case, but in this case, some refolding can be observed upon subsequent addition of excess DPC. At 37 °C, unfolding

[3] Attempts were also made to monitor the thermal denaturation of WT PMP22 using near-UV CD (not shown). The curve initially appears to be sigmoidal but loses this form past the midpoint. The detector voltage increases dramatically above 60 °C, suggesting aggregation above this temperature. Thermal irreversibility is a common phenomenon with membrane proteins studied in detergent micelles. Unfortunately, irreversibility prevents the extraction of meaningful thermodynamic parameters from the data, although it is apparent that PMP22 is stable up to ~50 °C.

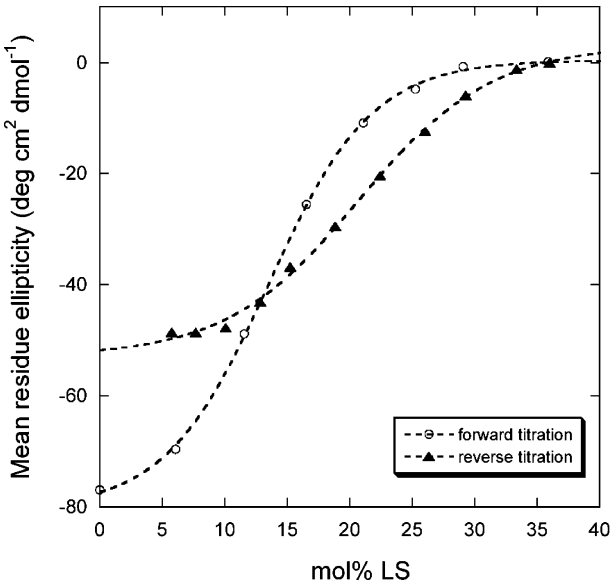

FIGURE 4: Forward (○) and reverse (▲) titrations of wild-type PMP22 in DPC micelles at 37 °C with the denaturing detergent laurylsarcosine, as monitored by CD at 299 nm. The buffer consisted of 25 mM acetate (pH 5.5), 150 mM NaCl, and 0.5% DPC with 10 mM Zn(II). Dashed lines represent fits of a two-state unfolding model (*38*).

using LS or SDS is complete in the dead time of the manual mixing (≤20 s).[4] Refolding of PMP22 from DPC/LS mixed micelles following addition of excess DPC occurs at 37 °C on a time scale of tens of minutes[5] (Figure 3C). There was a small burst phase signal, reflecting a rapid process that could not be observed with a manual mixing technique, which may be folding to an intermediate state. This is followed by much slower folding to the native state, a process that yields traces that can be fit to a single exponential. However, refolding is not 100% efficient, and the signal reaches only ~35% of its original value. These results indicate that the unfolding of PMP22 in model membranes is mostly irreversible in the absence of Zn(II). The reversibility increases to ~65% in the presence of Zn(II), as shown in the refolding traces in Figure 3C. Zn(II) clearly assists the folding of PMP22 in vitro.

Titration of Zn(II)-bound PMP22 with LS was followed by near-UV CD in both forward and reverse directions (Figure 4). The curves have the classic sigmoidal shape suggestive of a cooperative unfolding−refolding transition. However, the protein again could not be completely refolded by the addition of excess DPC, which was also observed in the kinetic refolding experiment. Since unfolding is not completely reversible, thermodynamic analysis is difficult. We attempted the experiment at other temperatures and pH values but did not find conditions that allowed complete reversal of unfolding. The maximum reversibility was 65% in the presence of Zn(II) and 35% in its absence.

[4] Unfolding was much faster at 37 °C that at 20 °C. For protein unfolding, k_{unfold} can vary over several orders of magnitude through a fairly narrow temperature range.

[5] Why does unfolding of PMP22 at 37 °C seem to be faster than the folding process? For a stable protein that unfolds via simple two-state kinetics, k_{fold} must be faster than k_{unfold}. However, PMP22 does not follow two-state kinetics, and there are at least two other rate constants (a burst phase fast folding rate constant and an irreversible unfolding rate constant), and while our refolding data provide a reasonable estimate of k_{fold}, we do not as of yet have a good estimate of k at low LS concentrations.

Under conditions of maximal reversibility, the forward unfolding curve and the backward refolding curve do not coincide, indicating hysteresis (Figure 4). Hysteresis most often occurs when slow kinetic steps that prevent a true equilibrium from being established are present. The presence of a slow folding transition and the observed difficulty of completely refolding PMP22 in these experiments appear to reflect a complex and difficult folding pathway, which may contribute to the inefficient folding observed in vivo.

Comparison of the Structure and Stability of WT PMP22 to Those of the Tr and TrJ Mutant Forms of PMP22. Two disease-linked mutant forms of PMP22, the Trembler (Tr, G150D) and Trembler-J (TrJ, L16P) mutants, were tested for their effects on the folding and stability of the protein. It is interesting to note that expression of these mutant forms of PMP22 in *E. coli* both slowed the growth of the host *E. coli* and led to much lower yields of the mutant proteins than WT PMP22 (data not shown).

Stability was first examined in the absence of Zn(II). Although the Tr and TrJ mutations have little apparent effect on PMP22's secondary structure (Figure 5A), L16P completely abrogates folded tertiary structure in DPC micelles (Figure 5B). G150D is intermediate between L16P and WT, indicating a destabilization of the native folded structure or an alteration of that structure. CD spectra in the presence of 10 mM Zn(II) showed that metal ion binding promoted the refolding of G150D into a nativelike tertiary fold but not L16P (Figure 6A). However, Zn(II)-bound G150D appears to be less stable than WT (see Figure 6B) and does not exhibit significant refolding after LS denaturation (data not shown). These results indicate that the Tr and TrJ mutant forms of PMP22 are significantly less stable than WT PMP22 in both the presence and absence of Zn(II). Moreover, in DPC micelles the Tr mutant of PMP22 is more stable than TrJ in both the absence and presence of Zn(II). Binding of Zn(II) led to folding of the Tr mutant (but not of TrJ) under conditions in which it was otherwise unfolded.

To assess the possibility that the Tr and TrJ mutations induce major changes in the structure of folded PMP22, we examined the $^1H-^{15}N$ TROSY NMR spectra of the L16P (TrJ) and G150D (Tr) mutant forms under conditions in which these proteins are folded in tetradecylphosphocholine (TDPC) micelles. As compared to the CD conditions involving dilute protein in DPC micelles, PMP22 is more stable in TDPC. Moreover, the higher protein concentrations in the NMR samples are expected to stabilize the dimeric form of the protein. The TROSY spectra of the mutants are shown in Figure 7 superimposed with the spectrum of WT. While the spectra of the mutants are somewhat noisy, the similarity of the spectra from both mutants to the spectrum of the wild-type protein is clear. While the possibility that the L16P (TrJ) and G150D (Tr) mutations induce moderate local conformational changes cannot be ruled out, these mutations clearly do not result in major global conformational changes in folded PMP22. The major effect of the mutations appears to be shifting the folding equilibrium away from the properly folded state.

DISCUSSION

Following translation and integration of nascent membrane proteins into the membrane of the ER by the translocon

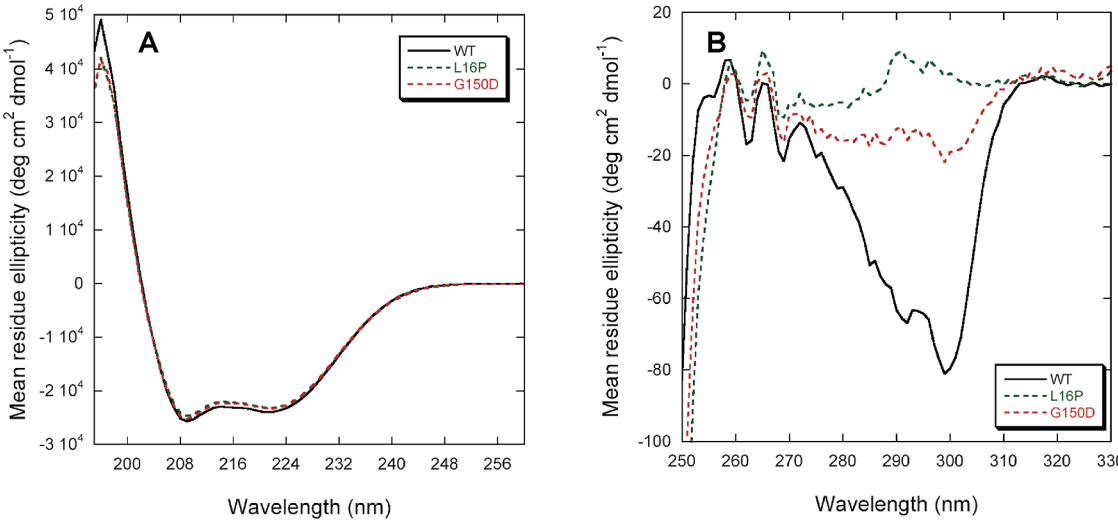

FIGURE 5: Circular dichroism spectra of the Tr (G150D) and TrJ (L16P) mutant forms of PMP22 in DPC micelles at 25 °C. (A) Far-UV CD spectra. (B) Near-UV CD spectra. The buffer consisted of 25 mM acetate (pH 5.5), 150 mM NaCl, and 0.5% DPC.

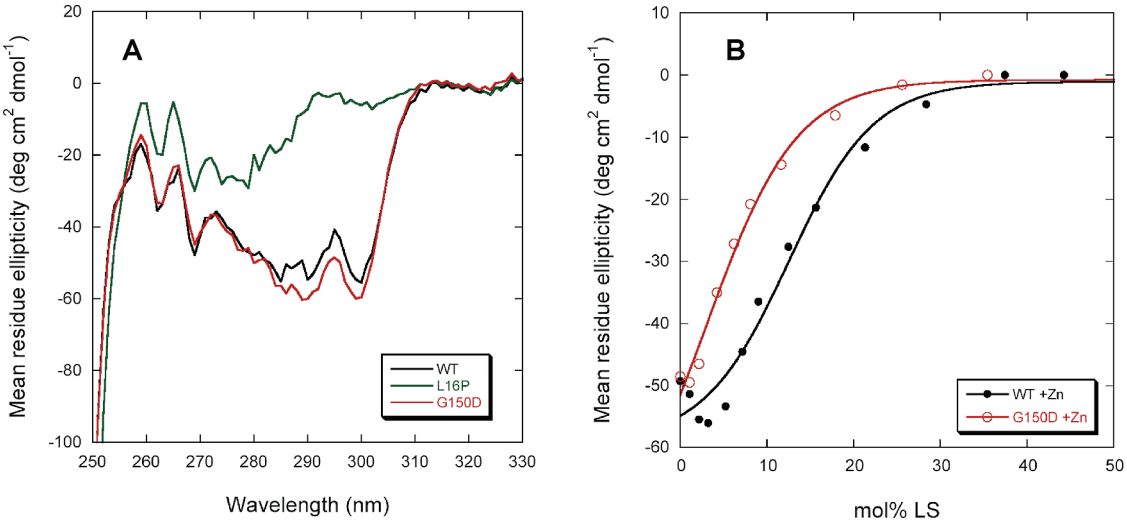

FIGURE 6: Properties of the Tr (G150D) and TrJ (L16P) mutant forms of PMP22 in the presence of Zn(II). (A) Near-UV CD spectra of the WT and mutants in the presence of 10 mM Zn(II). (B) Laurylsarcosine titrations followed by CD at 299 nm of WT and Tr PMP22 at 37 °C in the presence of Zn(II) showing the destabilization caused by the G150D mutation. The buffer consisted of 25 mM acetate (pH 5.5), 150 mM NaCl, and 0.5% DPC.

complex in eukaryotic cells, folding and misfolding is managed by the ER quality control system (*48*−*53*), which both assists the folding of nascent proteins and recognizes defective proteins, retaining them in the ER for further attempts to fold and/or potential degradation by the ERAD pathway. ERAD-targeted proteins are translocated back out of the ER into the cytosol, where they are typically polyubiquitinated and degraded by proteasomes.

The biophysical logic of ER quality control for membrane proteins is incompletely understood but has been postulated to be related to the thermal and kinetic stability of proteins that fold in the ER (reviewed in ref *48*). Proteins that are unstable or that fold only slowly may be particularly susceptible to being targeted for degradation by quality control. However, this possibility has been examined for only a few proteins, the majority of which are water soluble (*48, 54*).

For PMP22, there is a wealth of information available about the in vivo folding and trafficking efficiencies of both wild-type and mutant forms of the protein. Wild-type PMP22 appears to correctly fold and traffic with only modest efficiency, such that 80% of nascent PMP22 molecules are targeted for degradation via extrusion from the ER into the cytosol, polyubiquitination, and proteasomal degradation (*15, 55*). When proteasomal function is inhibited, degradation-targeted PMP22 forms perinuclear/centrosome-proximal aggresomes that are believed to normally be engulfed by autophagosomes and then degraded following delivery to the lysosomes (*20, 22*). It is known that most CMT1A-linked mutant forms of PMP22, including the Tr and TrJ mutants examined in this work, are targeted for degradation by ER quality control, with the efficiency of correct folding and trafficking approaching 0% (*17, 19, 24, 26, 27*). However, the nature of the defects in the disease mutants that are recognized by quality control is not well understood. Using cellular extracts, it has been shown that both the L16P (TrJ) and G150D (Tr) mutant forms of PMP22 are more prone than the WT protein to forming non-native aggregates (*23, 56*). However, it is unlikely that it is the aggregates themselves that are recognized and targeted for degradation by quality control; most likely, it is the formation of these very aggregates that quality control seeks to prevent (*48*).

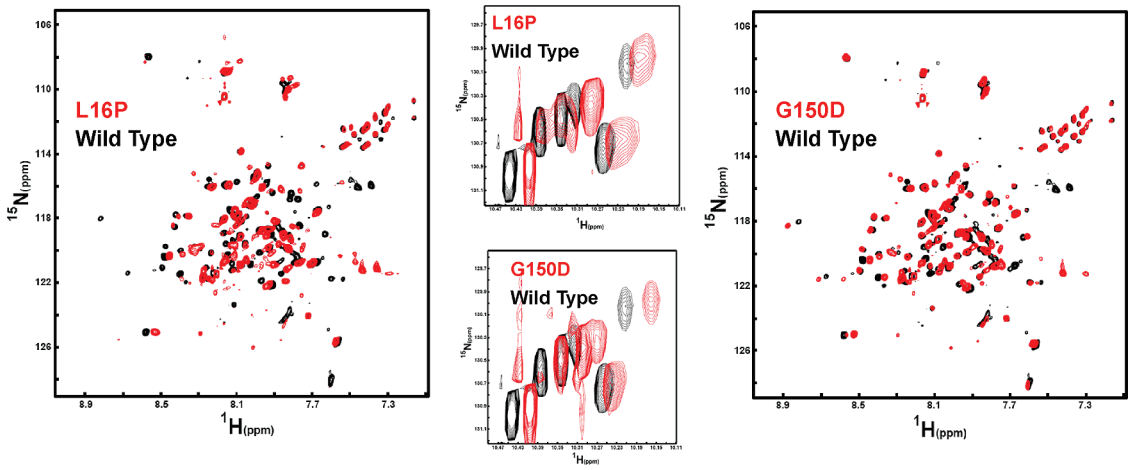

FIGURE 7: Comparison of the NMR spectrum for WT PMP22 in TDPC micelles to the spectra of the Tr (G150D) and TrJ (L16P) mutants under identical conditions [25 mM acetate (pH 5.5), 150 mM NaCl, and 0.2% TDPC]. All data were acquired at 800 MHz and 45 °C. In the left panel, the $^{1}H-^{15}N$ TROSY spectrum of the L16P PMP22 mutant (red) is overlaid on the spectrum of WT PMP22 (black). The L16P spectrum was collected using 128 increments and 248 scans per increment. The wild-type spectrum was collected with 128 increments and 180 scans. In the right panel, the $^{1}H-^{15}N$ TROSY spectrum of the G150D PMP22 mutant (red) is overlaid on the spectrum of WT PMP22 (black). Acquisition parameters for G150D were the same as those for L16P. In the center panel are shown mutant/WT TROSY spectral overlays for the indole ring $^{1}H-^{15}N$ from the protein's six tryptophan residues (five in PMP22 and one in the N-terminal tag).

One plausible mechanism by which quality control might recognize PMP22 as being folding-defective would be the detection of non-native structure in the protein. For example, the protein might form a molten globule-like conformational state that fails to complete folding to a fully ordered structure. Alternatively, the protein might adopt a non-native ordered fold. The NMR results of this paper do not support these possibilities. Under model membrane conditions in which wild-type PMP22 and the L16P and G150D mutants are each folded, the NMR spectra of these proteins strongly suggest that they have folded tertiary structures similar to that of WT.

For mutant forms of certain water soluble secretory proteins, it has been shown that the efficiency of folding and trafficking through the ER correlates with thermodynamic stability (reviewed in ref *48*). This suggests another property that might cue quality control that mutant forms of PMP22 are defective, the presence of long-lived populations of unfolded PMP22, reflecting thermodynamic instability and/or very slow folding kinetics. This possibility is supported by the results. The Tr and TrJ mutant forms of PMP22 were observed to be considerably less stable than the wild-type protein, as measured by denaturation with LS (Figure 4). The lower stabilities of the mutant forms of PMP22 correlate well with their reduced efficiency of productive folding and trafficking relative to those of the wild type under cellular conditions.

The observed instability of the Tr and TrJ mutants should not be taken to imply that after reaching a folding equilibrium in vivo in native ER membranes they prefer the unfolded state. Indeed, we were able to find micellar conditions under which these proteins were well-folded. However, stability, folding kinetics, and folding efficiency are interrelated. Reflecting the Haldane relationship, a reduction in protein stability is often coupled to a reduction in the protein folding rate. In this paper, we found that even wild-type PMP22 folded slowly in detergent micelles, requiring tens of minutes at 37 °C to reach completion, a prolonged process that is within 1 order of temporal magnitude of the protein's half-life in the cell (*16, 57*). Instability may also favor the formation of aggregation-prone non-native folding intermediates, leading to misfolding and low folding efficiency. It is known that even wild-type PMP22 folds in the cell and in micelles with much less than 100% efficiency. Moreover, this study shows that its in vitro folding is much slower than for most other multispan helical membrane proteins for which micellar refolding kinetic measurements have been taken (*16, 42, 43, 45, 57*−*61*), suggesting an unusually difficult folding pathway. While folding of PMP22 in the ER will be managed and facilitated in living cells by both the translocon and various chaperones, the fact that 80% of the nascent wild-type protein is targeted for degradation (*15, 55*) testifies to the fact that PMP22 is a difficult protein to fold even under highly evolved conditions. The extremely slow folding of wild-type PMP22 observed in this study suggests that the form of the protein that is principally recognized as defective and targeted for degradation by quality control in the ER could be nascent protein that has been integrated into the membrane but has not yet formed native tertiary structure. The fact that Tr and TrJ mutants are less stable (and more difficult to refold) than WT suggests that they likely fold even more slowly than WT, which would make these mutants even more vulnerable to recognition as being defective by quality control, leading to almost 100% targeting of the protein to degradative pathways.

The fact that the L16P and G150D mutant forms of PMP22 are less stable than the wild-type protein is not surprising. Leucine 16 is located midway through the first TM domain. Replacement of this residue with proline would most likely induce a kink in this helix that could disrupt tertiary structure. Indeed, missense mutation-encoded replacements of TM residues with proline are extremely common disease-linked mutations in membrane proteins (*62, 63*). It has previously been shown that the L16P (TrJ) mutant form of PMP22 forms long-lived complexes with calnexin, which is a chaperone that is central to ER quality control (*28, 57*). As for some other membrane proteins that form complexes with calnexin (*64*), the formation of this complex was found to be independent of glycosylation of the mutant PMP22, unlike that of the wild type. It was also found that the isolated first

transmembrane domain of both L16P and wild-type PMP22 binds avidly to calnexin (*57*). These results suggest that a key component of PMP22-specific quality control in the ER is the recognition by calnexin of the first transmembrane domain of PMP22, which is recognized only if it is not stably bundled with the other TM helices of the molecule. This is consistent with the notion that the L16P (Tr) mutation does indeed lead to the unfolding or failure of the protein to fold in a timely manner in the cell. The fact that the (defective) kink in the helix caused by L16P is not required for calnexin binding is demonstrated by the fact that calnexin binds to the isolated first TM segment of the wild-type protein (*57*). Whether calnexin actually serves as the primary folding sensor for PMP22-specific ER quality control has not yet been established.

The G150D (Tr) mutation would be expected to also destabilize the transmembrane domain by replacing a neutral residue located in the fourth TM segment with a charged amino acid. Moreover, this mutation involves replacement of an amino acid with liberal backbone conformational preferences (Gly) with one having more strict preferences (Asp). Interestingly, it is known that this mutant also forms prolonged complexes with calnexin (*28*), although it is not yet known whether this interaction is glycosylation-independent (as for TrJ) or whether binding involves the first TM segment.

PMP22 Is a Zn(II)-Binding Protein. A significant finding of this work is that PMP22 appears to bind both Zn(II) and Cu(II). Because membrane proteins tend to be better ordered in their native membrane then in a detergent micelle (*65*) and because PMP22's environment in compact myelin is very crowded, with only a modest (20 nm) extracellular gap separating apposed bilayers, the dissociation constant of 20 μM we measured for PMP22 and Zn(II) at neutral pH should be regarded as only an upper bound. Most likely, the binding to PMP22 will be tighter in the native environment, due to the coordinating side chains (most likely Cys and His in the extracellular loops) being more highly ordered.

BLAST searches of the human PMP22 sequence reveal no homology to any known Zn(II) binding protein, although the two Cys residues in the first extracellular loop appear to be part of a short sequence motif that is shared by PMP22 with several other tetraspan membrane proteins (*15*).

Is the binding of Zn(II) and/or Cu(II) to PMP22 physiologically relevant? Zn(II) and Cu(II) are known to be abundant in peripheral nervous system tissue, being present at ~200 and ~20 μM, respectively, in the rat sciatic nerve (*66*). Addition of Zn(II) is known to induce nativelike compaction of isolated myelin (*67*). The measured binding constant for Zn(II) and PMP22 at neutral pH is comparable to the binding constants measured for intracellular myelin-associated glycoprotein and myelin basic protein (*35*−*37*). Moreover, dietary Zn(II) deficiency induces changes in PNS myelination that resemble the defects observed in CMT1A (*33, 34*). However, the concentrations of Zn(II) or Cu(II) in the minimal extracellular space between the layers of myelin have not been measured, so our observation that purified PMP22 binds these ions in myelin must be regarded as merely suggestive.

Assuming that PMP22 does bind Zn(II) or Cu(II) in vivo, the metals might play a structural role in the extracellular loops, stabilizing a functionally important conformation. Alternatively, PMP22 may have evolved a particular functional role for the metal ion, possibly related to the interaction of PMP22 with itself, with MPZ, or with other myelin proteins (*68*). It is interesting to note that MPZ also appears to have an intrinsic affinity for Cu(II) metal ion affinity resin (*69*) and therefore may also bind Cu(II) and Zn(II). If Zn(II) is required for PMP22 function, then this likely contributes to the symptoms of zinc deficient rats (*33, 34*), which closely resemble the neuropathy arising from mutations in PMP22. Zn(II) or Cu(II) may also assist in PMP22 folding. The results of this work showed that for purified PMP22 the refolding efficiency doubled in the presence of Zn(II).

Conclusions. The Tr and TrJ mutations of PMP22 do not result in dramatic changes in the structure of PMP22 but result in the destabilization of the folded structure and depressed folding kinetics. It is possible that these are the defects that are recognized by ER quality control leading to targeting of these mutants for degradation. The associated phenotypes of DSS and CMT1A linked to these mutant forms are caused by the resulting loss of PMP22 function and, more importantly, by the toxic accumulation of these mutants and associated wild-type protein when the normally operative protein degradation systems fail. A number of other (but not all) phenotypes of CMT1A and related peripheral neuropathies are caused by other single-site mutations in PMP22, many of which are likely to induce defects in stability and folding kinetics similar to what was documented here for the Tr and TrJ mutants. Our observation that PMP22 can bind Zn(II) or Cu(II) suggests that the protein may bind these ions under physiological conditions.

REFERENCES

1. Bronstein, J. M. (2000) Function of tetraspan proteins in the myelin sheath. *Curr. Opin. Neurobiol. 10*, 552–557.
2. Quarles, R. H. (2002) Myelin sheaths: Glycoproteins involved in their formation, maintenance and degeneration. *Cell. Mol. Life Sci. 59*, 1851–1871.
3. Adlkofer, K., Martini, R., Aguzzi, A., Zielasek, J., Toyka, K. V., and Suter, U. (1995) Hypermyelination and demyelinating peripheral neuropathy in Pmp22-deficient mice. *Nat. Genet. 11*, 274–280.
4. Carenini, S., Neuberg, D., Schachner, M., Suter, U., and Martini, R. (1999) Localization and functional roles of PMP22 in peripheral nerves of P0-deficient mice. *Glia 28*, 256–264.
5. Taylor, V., Zgraggen, C., Naef, R., and Suter, U. (2000) Membrane topology of peripheral myelin protein 22. *J. Neurosci. Res. 62*, 15–27.
6. Mobley, C. K., Myers, J. K., Hadziselimovic, A., Ellis, C. D., and Sanders, C. R. (2007) Purification and initiation of structural characterization of human peripheral myelin protein 22, an integral membrane protein linked to peripheral neuropathies. *Biochemistry 46*, 11185–11195.
7. Van Itallie, C. M., and Anderson, J. M. (2006) Claudins and epithelial paracellular transport. *Annu. Rev. Physiol. 68*, 403–429.
8. Notterpek, L., Roux, K. J., Amici, S. A., Yazdanpour, A., Rahner, C., and Fletcher, B. S. (2001) Peripheral myelin protein 22 is a constituent of intercellular junctions in epithelia. *Proc. Natl. Acad. Sci. U.S.A. 98*, 14404–14409.
9. Takeda, Y., Notsu, T., Kitamura, K., and Uyemura, K. (2001) Functional analysis for peripheral myelin protein PASII/PMP22: Is it a member of claudin superfamily? *Neurochem. Res. 26*, 599–607.
10. Wilson, H. L., Wilson, S. A., Surprenant, A., and North, R. A. (2002) Epithelial membrane proteins induce membrane blebbing and interact with the P2X7 receptor C terminus. *J. Biol. Chem. 277*, 34017–34023.
11. Van Itallie, C. M., and Anderson, J. M. (2006) Claudins and epithelial paracellular transport. *Annu. Rev. Physiol. 68*, 403–429.

12. Berger, P., Niemann, A., and Suter, U. (2006) Schwann cells and the pathogenesis of inherited motor and sensory neuropathies (Charcot-Marie-Tooth disease). *Glia 54*, 243–257.
13. Jetten, A. M., and Suter, U. (2000) The peripheral myelin protein 22 and epithelial membrane protein family. *Prog. Nucleic Acid Res. Mol. Biol. 64*, 97–129.
14. Ryan, M. C., Shooter, E. M., and Notterpek, L. (2002) Aggresome formation in neuropathy models based on peripheral myelin protein 22 mutations. *Neurobiol. Dis. 10*, 109–118.
15. Sanders, C. R., Ismail-Beigi, F., and McEnery, M. W. (2001) Mutations of peripheral myelin protein 22 result in defective trafficking through mechanisms which may be common to diseases involving tetraspan membrane proteins. *Biochemistry 40*, 9453–9459.
16. Dickson, K. M., Bergeron, J. J., Shames, I., Colby, J., Nguyen, D. T., Chevet, E., Thomas, D. Y., and Snipes, G. J. (2002) Association of calnexin with mutant peripheral myelin protein-22 ex vivo: A basis for "gain-of-function" ER diseases. *Proc. Natl. Acad. Sci. U.S.A. 99*, 9852–9857.
17. Colby, J., Nicholson, R., Dickson, K. M., Orfali, W., Naef, R., Suter, U., and Snipes, G. J. (2000) PMP22 carrying the trembler or trembler-J mutation is intracellularly retained in myelinating Schwann cells. *Neurobiol. Dis. 7*, 561–573.
18. Young, P., and Suter, U. (2001) Disease mechanisms and potential therapeutic strategies in Charcot-Marie-Tooth disease. *Brain Res. Brain Res. Rev. 36*, 213–221.
19. D'Urso, D., Prior, R., Greiner-Petter, R., Gabreels-Festen, A. A., and Muller, H. W. (1998) Overloaded endoplasmic reticulum-Golgi compartments, a possible pathomechanism of peripheral neuropathies caused by mutations of the peripheral myelin protein PMP22. *J. Neurosci. 18*, 731–740.
20. Fortun, J., Dunn, W. A., Jr., Joy, S., Li, J., and Notterpek, L. (2003) Emerging role for autophagy in the removal of aggresomes in Schwann cells. *J. Neurosci. 23*, 10672–10680.
21. Fortun, J., Li, J., Go, J., Fenstermaker, A., Fletcher, B. S., and Notterpek, L. (2005) Impaired proteasome activity and accumulation of ubiquitinated substrates in a hereditary neuropathy model. *J. Neurochem. 92*, 1531–1541.
22. Fortun, J., Verrier, J. D., Go, J. C., Madorsky, I., Dunn, W. A., and Notterpek, L. (2007) The formation of peripheral myelin protein 22 aggregates is hindered by the enhancement of autophagy and expression of cytoplasmic chaperones. *Neurobiol. Dis. 25*, 252–265.
23. Liu, N., Yamauchi, J., and Shooter, E. M. (2004) Recessive, but not dominant, mutations in peripheral myelin protein 22 gene show unique patterns of aggregation and intracellular trafficking. *Neurobiol. Dis. 17*, 300–309.
24. Naef, R., and Suter, U. (1999) Impaired intracellular trafficking is a common disease mechanism of PMP22 point mutations in peripheral neuropathies. *Neurobiol. Dis. 6*, 1–14.
25. Notterpek, L., Ryan, M. C., Tobler, A. R., and Shooter, E. M. (1999) PMP22 accumulation in aggresomes: Implications for CMT1A pathology. *Neurobiol. Dis. 6*, 450–460.
26. Tobler, A. R., Notterpek, L., Naef, R., Taylor, V., Suter, U., and Shooter, E. M. (1999) Transport of Trembler-J mutant peripheral myelin protein 22 is blocked in the intermediate compartment and affects the transport of the wild-type protein by direct interaction. *J. Neurosci. 19*, 2027–2036.
27. Tobler, A. R., Liu, N., Mueller, L., and Shooter, E. M. (2002) Differential aggregation of the Trembler and Trembler J mutants of peripheral myelin protein 22. *Proc. Natl. Acad. Sci. U.S.A. 99*, 483–488.
28. Dickson, K. M., Bergeron, J. J. M., Shames, I., Colby, J., Nguyen, D. T., Chevet, E., Thomas, D. Y., and Snipes, G. J. (2002) Association of calnexin with mutant peripheral myelin protein-22 ex vivo: A basis for "gain-of-function" ER diseases. *Proc. Natl. Acad. Sci. U.S.A. 99*, 9852–9857.
29. Sedzik, J., Kotake, Y., and Uyemura, K. (1998) Purification of PASII/PMP22: An extremely hydrophobic glycoprotein of PNS myelin membrane. *NeuroReport 9*, 1595–1600.
30. Sedzik, J., Uyemura, K., and Tsukihara, T. (2002) Towards crystallization of hydrophobic myelin glycoproteins: P0 and PASII/PMP22. *Protein Expression Purif. 26*, 368–377.
31. Frederickson, C. J., Suh, S. W., Silva, D., Frederickson, C. J., and Thompson, R. B. (2000) Importance of zinc in the central nervous system: The zinc-containing neuron. *J. Nutr. 130*, 1471S–1483S.
32. Que, E. L., Domaille, D. W., and Chang, C. J. (2008) Metals in neurobiology: Probing their chemistry and biology with molecular imaging. *Chem. Rev. 108*, 1517–1549.
33. Unal, B., Tan, H., Orbak, Z., Kiki, I., Bilici, M., Bilici, N., Aslan, H., and Kaplan, S. (2005) Morphological alterations produced by zinc deficiency in rat sciatic nerve: A histological, electron microscopic, and stereological study. *Brain Res. 1048*, 228–234.
34. Gong, H., and Amemiya, T. (2001) Optic nerve changes in zinc-deficient rats. *Exp. Eye Res. 72*, 363–369.
35. Kursula, P., Merilainen, G., Lehto, V. P., and Heape, A. M. (1999) The small myelin-associated glycoprotein is a zinc-binding protein. *J. Neurochem. 73*, 2110–2118.
36. Riccio, P., Giovannelli, S., Bobba, A., Romito, E., Fasano, A., Bleve-Zacheo, T., Favilla, R., Quagliariello, E., and Cavatorta, P. (1995) Specificity of zinc binding to myelin basic protein. *Neurochem. Res. 20*, 1107–1113.
37. Tsang, D., Tsang, Y. S., Ho, W. K., and Wong, R. N. (1997) Myelin basic protein is a zinc-binding protein in brain: Possible role in myelin compaction. *Neurochem. Res. 22*, 811–819.
38. Pace, C. N., and Scholtz, J. M. (1997) Measuring the conformational stability of a protein. In *Protein Structure: A Practical Approach* (Creighton, T. E., Ed.) pp 299−321, IRL Press, Oxford, U.K.
39. Weigelt, J., Miles, C. S., Dixon, N. E., and Otting, G. (1998) Backbone NMR assignments and secondary structure of the N-terminal domain of DnaB helicase from *E. coli*. *J. Biomol. NMR 11*, 233–234.
40. Lau, F. W., and Bowie, J. U. (1997) A method for assessing the stability of a membrane protein. *Biochemistry 36*, 5884–5892.
41. Sehgal, P., Mogensen, J. E., and Otzen, D. E. (2005) Using micellar mole fractions to assess membrane protein stability in mixed micelles. *Biochim. Biophys. Acta 1716*, 59–68.
42. Lorch, M., and Booth, P. J. (2004) Insertion kinetics of a denatured α helical membrane protein into phospholipid bilayer vesicles. *J. Mol. Biol. 344*, 1109–1121.
43. Nagy, J. K., and Sanders, C. R. (2004) Destabilizing mutations promote membrane protein misfolding. *Biochemistry 43*, 19–25.
44. Mackenzie, K. R. (2006) Folding and stability of α-helical integral membrane proteins. *Chem. Rev. 106*, 1931–1977.
45. Seddon, A. M., Curnow, P., and Booth, P. J. (2004) Membrane proteins, lipids and detergents: Not just a soap opera. *Biochim. Biophys. Acta 1666*, 105–117.
46. Stanley, A. M., and Fleming, K. G. (2008) The process of folding proteins into membranes: Challenges and progress. *Arch. Biochem. Biophys. 469*, 46–66.
47. Popot, J. L., and Engelman, D. M. (1990) Membrane protein folding and oligomerization: The two-stage model. *Biochemistry 29*, 4031–4037.
48. Sanders, C. R., and Myers, J. K. (2004) Disease-related misassembly of membrane proteins. *Annu. Rev. Biophys. Biomol. Struct. 33*, 25–51.
49. Krebs, M. P., Noorwez, S. M., Malhotra, R., and Kaushal, S. (2004) Quality control of integral membrane proteins. *Trends Biochem. Sci. 29*, 648–655.
50. Helenius, A., and Aebi, M. (2004) Roles of N-linked glycans in the endoplasmic reticulum. *Annu. Rev. Biochem. 73*, 1019–1049.
51. Anelli, T., and Sitia, R. (2008) Protein quality control in the early secretory pathway. *EMBO J. 27*, 315–327.
52. Brodsky, J. L. (2007) The protective and destructive roles played by molecular chaperones during ERAD (endoplasmic-reticulum-associated degradation). *Biochem. J. 404*, 353–363.
53. Hebert, D. N., and Molinari, M. (2007) In and out of the ER: Protein folding, quality control, degradation, and related human diseases. *Physiol. Rev. 87*, 1377–1408.
54. Wiseman, R. L., Koulov, A., Powers, E., Kelly, J. W., and Balch, W. E. (2007) Protein energetics in maturation of the early secretory pathway. *Curr. Opin. Cell Biol. 19*, 359–367.
55. Pareek, S., Notterpek, L., Snipes, G. J., Naef, R., Sossin, W., Laliberte, J., Iacampo, S., Suter, U., Shooter, E. M., and Murphy, R. A. (1997) Neurons promote the translocation of peripheral myelin protein 22 into myelin. *J. Neurosci. 17*, 7754–7762.
56. Tobler, A. R., Liu, N., Mueller, L., and Shooter, E. M. (2002) Differential aggregation of the Trembler and Trembler J mutants of peripheral myelin protein 22. *Proc. Natl. Acad. Sci. U.S.A. 99*, 483–488.
57. Fontanini, A., Chies, R., Snapp, E. L., Ferrarini, M., Fabrizi, G. M., and Brancolini, C. (2005) Glycan-independent role of calnexin in the intracellular retention of Charcot-Marie-tooth 1A Gas3/PMP22 mutants. *J. Biol. Chem. 280*, 2378–2387.
58. Booth, P. J., Templer, R. H., Meijberg, W., Allen, S. J., Curran, A. R., and Lorch, M. (2001) In vitro studies of membrane protein folding. *Crit. Rev. Biochem. Mol. Biol. 36*, 501–603.

59. Nagy, J. K., Lonzer, W. L., and Sanders, C. R. (2001) Kinetic study of folding and misfolding of diacylglycerol kinase in model membranes. *Biochemistry 40*, 8971–8980.
60. Otzen, D. E. (2003) Folding of DsbB in mixed micelles: A kinetic analysis of the stability of a bacterial membrane protein. *J. Mol. Biol. 330*, 641–649.
61. Tamm, L. K., Hong, H., and Liang, B. (2004) Folding and assembly of β-barrel membrane proteins. *Biochim. Biophys. Acta 1666*, 250–263.
62. Partridge, A. W., Therien, A. G., and Deber, C. M. (2004) Missense mutations in transmembrane domains of proteins: Phenotypic propensity of polar residues for human disease. *Proteins 54*, 648–656.
63. Sanders, C. R. (2005) Post-integration misassembly of membrane protein and disease. In *Protein-Lipid Interactions* (Tamm, L. K., Ed.) pp 81−94, Wiley-VCH, Weinheim, Germany.
64. Korkhov, V. M., Milan-Lobo, L., Zuber, B., Farhan, H., Schmid, J. A., Freissmuth, M., and Sitte, H. H. (2008) Peptide-based interactions with calnexin target misassembled membrane proteins into endoplasmic reticulum-derived multilamellar bodies. *J. Mol. Biol. 378*, 337–352.
65. Bond, P. J., and Sansom, M. S. (2003) Membrane protein dynamics versus environment: Simulations of OmpA in a micelle and in a bilayer. *J. Mol. Biol. 329*, 1035–1053.
66. Cloez, I., and Bourre, J. M. (1987) Copper, manganese and zinc in the developing brain of control and quaking mice. *Neurosci. Lett. 83*, 118–122.
67. Inouye, H., and Kirschner, D. A. (1984) Effects of $ZnCl_2$ on membrane interactions in myelin of normal and shiverer mice. *Biochim. Biophys. Acta 776*, 197–208.
68. D'Urso, D., Ehrhardt, P., and Muller, H. W. (1999) Peripheral myelin protein 22 and protein zero: A novel association in peripheral nervous system myelin. *J. Neurosci. 19*, 3396–3403.
69. Sedzik, J., Kotake, Y., and Uyemura, K. (1999) Purification of P0 myelin glycoprotein by a Cu^{2+}-immobilized metal affinity chromatography. *Neurochem. Res. 24*, 723–732.

BI801157P